

# Pulmonary Vasculitis

Melanie B. Peachell, M.D.<sup>1</sup> and Nestor L. Müller, M.D., Ph.D.<sup>1</sup>

## ABSTRACT

This review summarizes the radiological manifestations of the vasculitides of proven or presumed immunologic origin in which the inflammatory reaction is directed primarily against the vessel wall. These include Wegener's granulomatosis, Churg-Strauss syndrome, Takayasu's arteritis, Behçet's syndrome, Goodpasture's syndrome, and microscopic polyangiitis. Chest radiography is used routinely in the initial evaluation and follow-up of these patients. The radiographic findings however are nonspecific and need to be interpreted together with the clinical findings. Computed tomography (CT) plays an increasingly important role in the assessment of patients with vasculitis and, in the proper clinical context, allows a confident diagnosis of some of these entities. Magnetic resonance imaging and positron emission tomography play a limited role. The characteristic imaging manifestations of the various vasculitides are reviewed and illustrated.

**KEYWORDS:** Lung diseases, vasculitis, lung radiography, lung CT

**Objectives:** Upon completion of this article, the reader will understand: (1) the main radiographic manifestations of pulmonary vasculitis; (2) the computed tomographic findings of pulmonary vasculitis; and (3) the limitations and indications of imaging in the assessment of patients with suspected or proven pulmonary vasculitis.

**Accreditation:** The University of Michigan is accredited by the Accreditation Council for Continuing Medical Education to sponsor continuing medical education for physicians.

**Credits:** The University of Michigan designates this educational activity for a maximum of 1 category 1 credit toward the AMA Physician's Recognition Award.

The pulmonary vasculitides encompass a heterogeneous group of diseases that can affect the pulmonary arteries, veins, and capillaries. They include idiopathic vasculitides, diffuse hemorrhage syndromes, secondary forms of vasculitis, and miscellaneous systemic disorders.<sup>1</sup>

Chest radiography and computed tomography (CT) play an important role in the initial evaluation and follow-up of patients with clinically suspected pulmonary vasculitis. This article reviews the radiological manifestations of the vasculitides of proven or presumed immunologic origin in which the inflammatory reaction

is directed primarily against the vessel wall. These include Wegener's granulomatosis, Churg-Strauss syndrome, Takayasu's arteritis, Behçet's syndrome, Goodpasture's syndrome, and microscopic polyangiitis. Idiopathic vasculitis syndromes that rarely affect the lung, such as polyarteritis nodosa; cryoglobulinemic vasculitis and hypocomplementemic vasculitis; pulmonary vasculitis associated with connective tissue disease, such as lupus erythematosus; and vasculitis secondary to infection, drugs, or irradiation are beyond the scope of this review.

Pulmonary Vasculitis; Editor in Chief, Joseph P. Lynch, III, M.D.; Guest Editor, Carol A. Langford, M.D., M.H.S. *Seminars in Respiratory and Critical Care Medicine*, volume 25, number 5, 2004. Address for correspondence and reprint requests: Dr. Nestor L. Müller, Department of Radiology, Vancouver General Hospital, 899 W. 12<sup>th</sup> Ave., Vancouver, BC, Canada V5Z 1M9. E-mail: nmuller@vanhosp.bc.ca. <sup>1</sup>Department of Radiology, Vancouver General Hospital, University of British Columbia, Vancouver, British Columbia, Canada. Copyright © 2004 by Thieme Medical Publishers, Inc., 333 Seventh Avenue, New York, NY 10001, USA. Tel: +1(212) 584-4662. 1069-3424,p;2004,25,05,483,489, ftx,en;srm00323x.

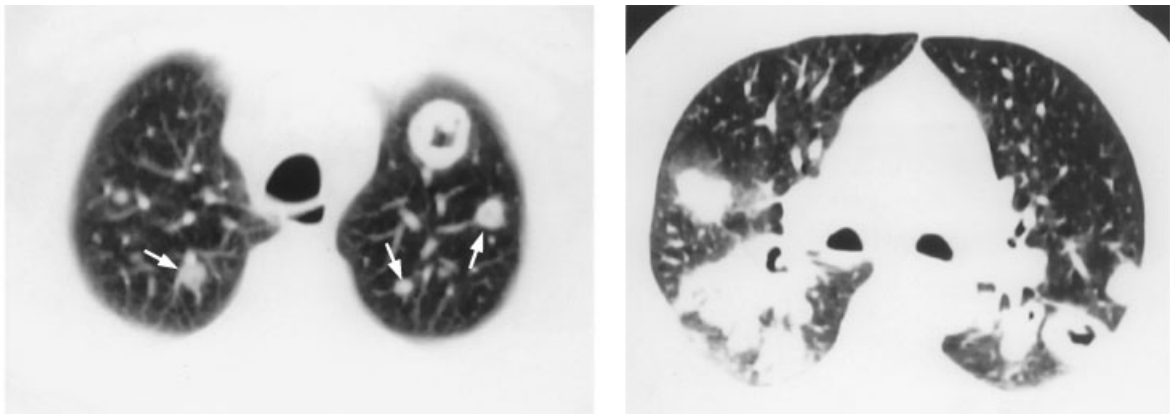


**Figure 1** Wegener's granulomatosis. (A) Computed tomographic (CT) scan at the level of the upper lobes shows bilateral noncavitating nodules (arrows) in the apical regions of both lungs and a cavitating nodule in the left apex. (B) CT scan at the level of main stem bronchi shows multiple cavitating and noncavitating nodules mainly in the subpleural and peribronchovascular regions. The patient was a 50-year-old man.

### WEGENER'S GRANULOMATOSIS

Wegener's Granulomatosis (WG) is a systemic granulomatous inflammatory process with variable clinical expression. It classically involves the upper and lower respiratory tracts and kidneys. In some patients it can be manifested primarily or exclusively in the respiratory tract, a form known as limited (nonrenal) WG. The characteristic pathological findings of WG include necrotizing granulomata of the respiratory tract, necrotizing vasculitis affecting medium to small pulmonary arteries and veins, and a focal glomerulonephritis.<sup>1</sup>

The most common radiological manifestation of pulmonary WG consists of multiple nodules.<sup>2-4</sup> The nodules range from 0.3 to 10 cm in diameter and are usually bilateral.<sup>5</sup> The nodules may be smooth or spiculated; ~50% eventually demonstrate cavitation.<sup>6</sup> The cavities typically have thick walls and shaggy, irregular inner borders<sup>7</sup> (Fig. 1). As the disease progresses, the nodules tend to increase in size and number.<sup>8</sup> CT is superior to chest radiographs in demonstrating the presence and number of nodules and presence of cavitation.<sup>6</sup> Cavitation usually occurs in nodules > 2 cm in diameter.<sup>6</sup> In one review of the CT findings in 30 patients, 27 (90%) had nodules or masses; cavitation of one or more of the nodules was present in 13 (48%) of these 27 patients.<sup>4</sup> The nodules ranged from 1 to 32 in number (mean 8) and had a predominantly subpleural or peribronchial distribution.<sup>4</sup>

Another common radiological finding is the presence of areas of air space consolidation or ground-glass opacities<sup>7</sup> (Fig. 2). These are seen in ~50% of patients.<sup>7</sup> Several patterns of distribution of the areas of consolidation and ground-glass opacification have been described, including diffuse, wedge-shaped pleural based, peribronchial, and patchy<sup>7,9</sup> (Fig. 3). Diffuse consolidation or ground-glass attenuation is seen in ~8% of patients and usually reflects the presence of diffuse pulmonary hemorrhage.<sup>5</sup> The areas of consolidation may be seen

in association with pulmonary nodules or as an isolated finding; in ~15% of patients cavitation is evident radiologically within the areas of consolidation.<sup>5</sup> Occasionally, foci of calcification may be seen within areas of consolidation and nodules.<sup>7</sup>

Tracheobronchial involvement occurs in ~30 to 50% of patients with WG.<sup>4,5</sup> Rarely, tracheobronchial abnormalities may be the only site of involvement or be the presenting abnormality in WG.<sup>10,11</sup> The most common manifestations are tracheobronchitis, tracheal or bronchial stenosis, and subglottic stenosis.<sup>5,12</sup> The stenosis tends to be focal and most commonly involves the main bronchi followed by the trachea, bronchus intermedius, and lower lobar bronchi.<sup>5</sup> CT demonstrates thickening of the airway wall and associated luminal narrowing.<sup>7,13</sup> The severity and extent of airway narrowing are best evaluated using multiplanar and

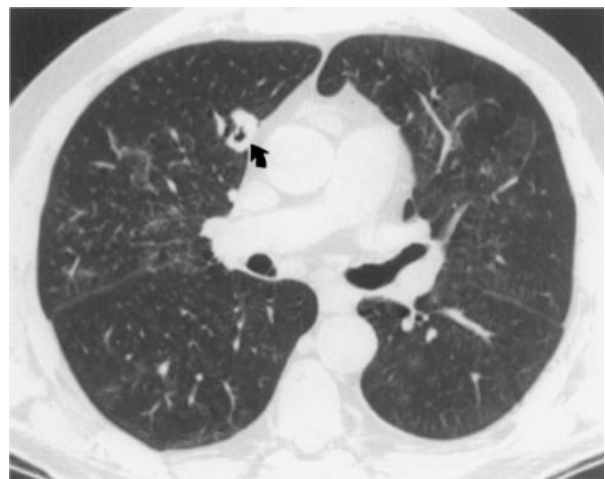


**Figure 2** Wegener's granulomatosis. Computed tomographic scan image at the level of the right main pulmonary artery shows poorly defined bilateral ground glass opacities and a cavitating nodule (arrow) in the right middle lobe. The ground-glass opacities were due to diffuse pulmonary hemorrhage. The patient was a 53-year-old man.



**Figure 3** Wegener's granulomatosis. Computed tomographic scan image at the level of the inferior pulmonary veins shows bilateral areas of consolidation in a peribronchovascular distribution. The patient was a 35-year-old woman.

three-dimensional reconstructions of spiral CT scans performed using thin sections.<sup>7,13</sup> Bronchial narrowing and obstruction may result in distal atelectasis. Bronchiectasis may occur with or without associated parenchymal manifestations of WG.<sup>8</sup> Less common findings include intra- and extraluminal soft tissue masses and calcification of the tracheal rings.<sup>4,10</sup>

Pleural effusions are seen in ~12 to 25% of patients and may be unilateral or bilateral, small or large.<sup>2-5,14</sup> Other pleural abnormalities that can rarely be seen include unilateral or bilateral pleural thickening, pneumothorax, hydropneumothorax, or pyopneumothorax.<sup>3,7,6</sup> Mediastinal lymph node enlargement is evident on CT in 20% of patients.<sup>4</sup>

### TAKAYASU'S ARTERITIS

Takayasu's arteritis is an uncommon arteritis that affects the aorta and its proximal branches and, less commonly, the pulmonary arteries. Approximately 90% of cases occur in women and the majority of cases occur in Southeast Asia.<sup>15,16</sup>

The chest radiograph is frequently normal or shows nonspecific findings, including a scalloped contour of the descending thoracic aorta, ectasia of the arch, dilatation of the ascending aorta, and aortic calcification in a young patient.<sup>17</sup> CT is usually abnormal and, in the appropriate clinical setting, often allows confident diagnosis.

The findings on CT are best evaluated by performing CT before and after intravenous administration of contrast. CT without intravenous contrast typically demonstrates thickening and high attenuation of the involved vessel wall, usually the thoracic aorta or brachiocephalic artery, and, frequently, mural calcification.<sup>18</sup> The thickened wall shows enhancement following intravenous administration of contrast<sup>18</sup> (Fig. 4). Enhancement of the vessel wall following

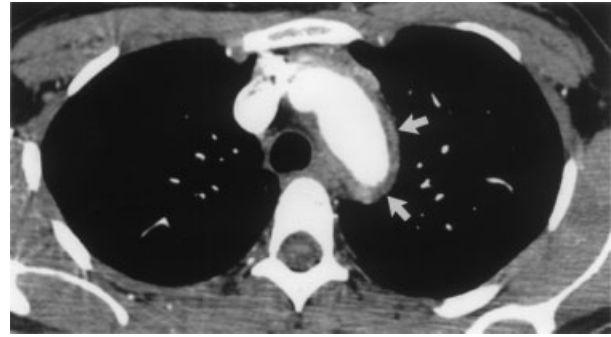


**Figure 4** Takayasu's arteritis. Computed tomographic image obtained following intravenous administration of contrast demonstrates thickening and enhancement of the wall of the aorta at the level of the aortic arch (arrows). The patient was a 32-year-old woman.

intravenous administration of contrast and the presence of an inner hypoattenuating rim are typically seen in patients with active disease.<sup>18</sup> Patients with longstanding but inactive disease tend to show high attenuation and calcification of the arterial walls on the precontrast images and lack of mural enhancement on the postcontrast images.<sup>18</sup> Involvement of the arterial wall can result in focal areas of stenosis or aneurysm formation. The most frequent site of stenosis is in the descending aorta whereas aneurysms are more commonly seen in the ascending aorta.<sup>19</sup>

The pulmonary arteries are involved in 50 to 86% of patients and on CT demonstrate increased wall thickness and mural enhancement.<sup>16,18</sup> The vast majority of patients with pulmonary arterial involvement have concomitant involvement of the aorta or its branches.<sup>18</sup> Pulmonary parenchymal abnormalities have been described. In a recent retrospective study, 10 of 20 patients with Takayasu's were found to have areas of decreased pulmonary parenchymal attenuation and vascularity on HCRT (high resolution computed tomography).<sup>20</sup> The low attenuation areas were consistent with localized hypoperfusion, presumably secondary to pulmonary arteritis.

In the majority of patients the diagnosis of Takayasu's arteritis is made based on the clinical and CT findings. Magnetic resonance imaging (MRI) can also be useful. MRI can demonstrate the presence of wall thickening of the involved vessels, stenosis, and aneurysm formation.<sup>19,21</sup> MRI may be particularly helpful in demonstrating vascular anatomy in patients being evaluated in centers where spiral CT is not available. One case has been reported where positron emission tomography (PET) with fluorodeoxyglucose (FDG-PET) was useful in the early diagnosis of Takayasu's.<sup>22</sup> Increased uptake of FDG in Takayasu's reflects the presence of marked inflammation of the vessel wall in the early stages of Takayasu's arteritis.<sup>22</sup>

## CHURG-STRAUSS SYNDROME

Churg-Strauss syndrome is a rare condition seen almost exclusively in patients with asthma and characterized by the presence of systemic vasculitis, extravascular granulomatous inflammation, and eosinophilia.<sup>23,24</sup>

The most common radiological manifestations consist of transient, patchy, nonsegmental areas of consolidation without predilection for any lung zone.<sup>24-26</sup> The areas of consolidation can be symmetric or asymmetric and may have a peripheral distribution similar to that seen in chronic eosinophilic pneumonia<sup>25,26</sup> (Fig. 5). Less common manifestations include small or large nodules, unilateral or bilateral pleural effusions, and hilar lymphadenopathy.

High-resolution CT frequently demonstrates bilateral ground-glass opacities with or without associated areas of consolidation. In one review of the high-resolution CT findings in 17 patients, 11 (60%) had areas of ground-glass attenuation or consolidation in either a patchy or a predominantly peripheral distribution.<sup>27</sup> Two patients had small centrilobular nodules, two had multiple nodules measuring 0.5 to 3.5 cm in diameter, and one had interlobular septal thickening. Similar findings were reported in a second study of nine patients with Churg-Strauss syndrome.<sup>24</sup>

Interlobular septal thickening and small effusions in patients with Churg-Strauss syndrome may be secondary to cardiac involvement or, occasionally, be seen in patients with Churg-Strauss Syndrome and normal cardiac function<sup>27</sup> (Fig. 6). A single case has been reported in which high-resolution CT demonstrated enlarged peripheral arteries, some of which had an irregular, stellate configuration and which correlated with the presence of vasculitis histologically.<sup>28</sup> Pleural effusions are seen on CT in ~30% of cases.<sup>16</sup> Hilar and mediastinal lymphadenopathy can occur but are uncommon.

## BEHÇET'S DISEASE

Behçet's disease is a rare chronic, multisystem disease characterized by the presence of uveitis and oral and genital ulcers. It occurs most commonly in the Middle East and Japan and affects men more commonly than women.<sup>29</sup> Thoracic vascular involvement occurs in 25% of patients and pulmonary manifestations in ~5%.<sup>29-31</sup>

The most common thoracic manifestations of Behçet's disease are narrowing or thrombosis of the superior vena cava, pulmonary artery aneurysms, pulmonary hemorrhage, and pulmonary infarction.<sup>32,33</sup> Thrombosis of the superior vena cava is manifested radiologically by the presence of widening of the mediastinum.

Pulmonary artery aneurysms are manifested radiographically by the presence of single or multiple round perihilar opacities or rapidly progressive unilateral hilar enlargement.<sup>29,32</sup> The aneurysms may be single or multiple, unilateral or bilateral, and measure 1 to 7 cm in diameter.<sup>32,34,35</sup> Aneurysm formation is more commonly seen on the right (59%) and in the lobar arteries (54%).<sup>35</sup> The right lower lobe artery is the most commonly affected (35%) followed by the left lower lobe and right main pulmonary arteries<sup>35</sup> (Fig. 7). The presence, size, and location of pulmonary artery aneurysms can be assessed with CT and MRI.<sup>32,35,36</sup> Conventional angiography is not recommended in the imaging of patients with Behçet's disease because catheter insertion may lead to venous thrombosis or aneurysm formation at the site of puncture.

Pulmonary artery aneurysms can increase in size and rupture, leading to pulmonary hemorrhage and death, or regress spontaneously with treatment.<sup>32,33,35</sup> Pulmonary hemorrhage can result in focal, multifocal, or diffuse airspace consolidation.<sup>29,34</sup> Thrombotic occlusion of the aneurysmal pulmonary artery can result in localized areas of consolidation secondary to pulmonary infarction, areas of oligemia, and areas of atelectasis.<sup>34,37</sup>

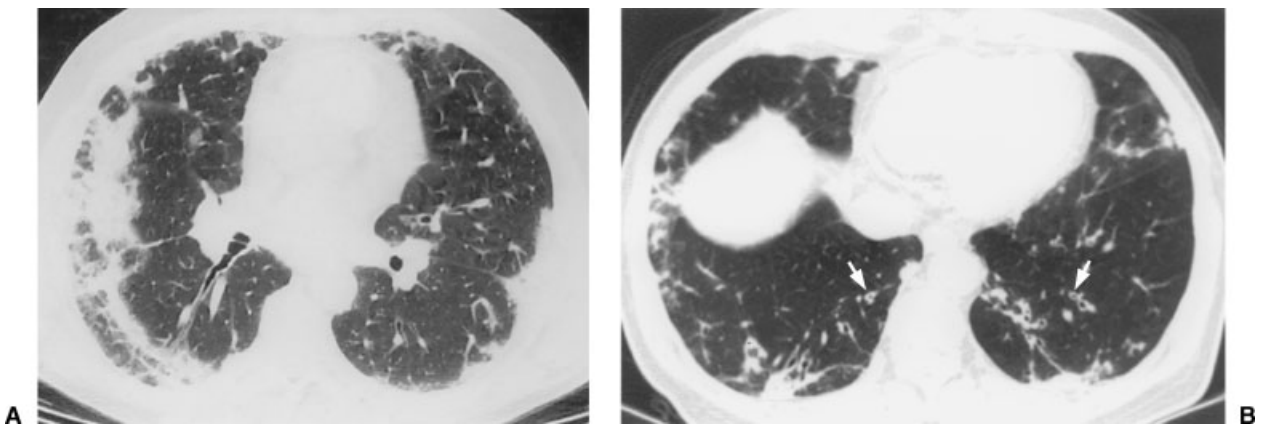


**Figure 5** Churg-Strauss Syndrome. (A) Computed tomographic (CT) scan at the level of the inferior pulmonary veins shows patchy bilateral areas of consolidation involving mainly the peripheral regions of the lower lobes. (B) CT scan at the level of the right hemidiaphragm shows bronchial wall thickening (arrows) and patchy peripheral areas of consolidation in the lower lobes. The patient was a 52-year-old man.



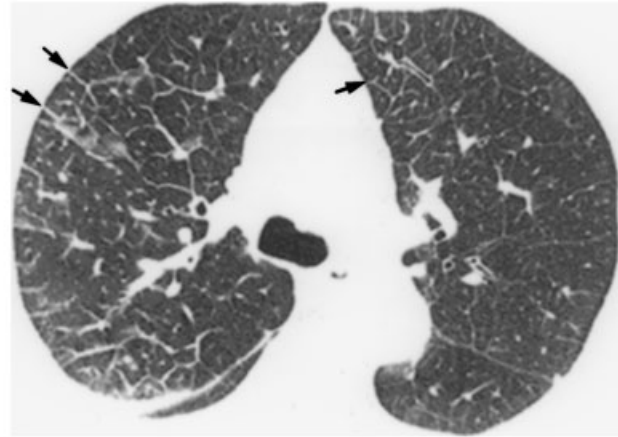


**Figure 6** Churg-Strauss Syndrome. (A) Posteroanterior chest radiograph shows small bilateral lower lobe consolidation, linear opacities, and small pleural effusions. (B) Computed tomographic image at the level of the carina demonstrates smooth thickening of the interlobular septa (arrows). The patient was a 69-year-old woman with no clinical or echocardiographic evidence of left heart failure. The septal thickening was due to pulmonary involvement.

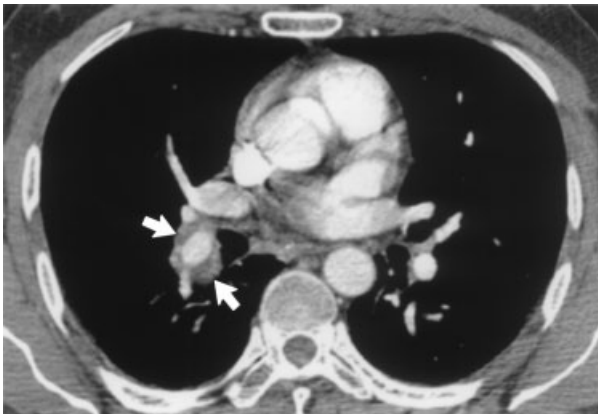


**Figure 7** Behçet's disease. Computed tomographic image at the level of the superior pulmonary veins demonstrates circumferential nonocclusive thrombus within an aneurysm of the right interlobar artery (arrows). The patient was a 48-year-old man.

### GOODPASTURE'S SYNDROME

Goodpasture's syndrome is a pulmonary-renal syndrome characterized by the presence of antiglomerular basement membrane antibodies in the circulation.<sup>38</sup> It affects both the kidneys and the lungs in 60 to 80% of cases, only the kidneys in 20 to 40%, and only the lungs in < 10% of cases.<sup>39</sup> It is seen most commonly in young adults (mean age 35 years) and is more common in males than females.

The radiological manifestations reflect the presence of diffuse pulmonary hemorrhage and consist of patchy or confluent bilateral areas of consolidation.<sup>40</sup> The consolidation can be diffuse but tends to involve mainly the perihilar regions and spare the lung apices and the costophrenic angles.<sup>40,41</sup> Less common findings include ground-glass opacities and migratory areas of consolidation<sup>41</sup> (Fig. 8). The chest radiograph, however,

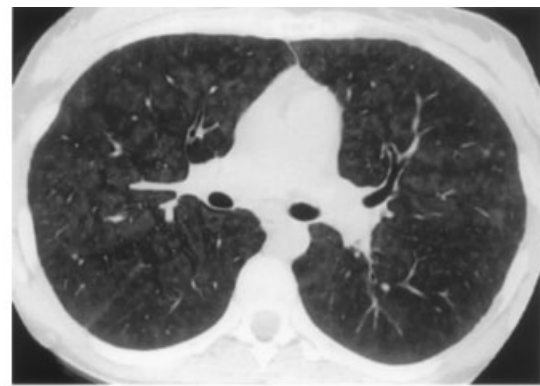


**Figure 8** Goodpasture's syndrome. (A) Computed tomographic (CT) image at the level of the aortic arch shows centrilobular ground-glass opacities throughout the upper lobes due to diffuse pulmonary hemorrhage. (B) CT image at the level of the right main pulmonary artery shows ground-glass opacities in the lower lobes. The patient was a 35-year-old woman.

can be normal in the setting of diffuse pulmonary hemorrhage.<sup>40</sup> In one review of 39 patients, Bowley et al found the chest radiograph to be normal in 7 (18%) cases.<sup>40</sup> The CT manifestations of acute pulmonary hemorrhage consist of bilateral ground-glass opacities or areas of consolidation. These can be patchy or diffuse but tend to involve predominantly the dependent lung regions.<sup>41,42</sup>

### MICROSCOPIC POLYANGIITIS

Microscopic polyangiitis is a systemic disease characterized by necrotizing vasculitis with few or no immune deposits that involves predominantly or exclusively the arterioles, venules, and capillaries.<sup>1</sup> The most common clinical manifestations are glomerulonephritis, dyspnea, cough, hemoptysis, fever, myalgia, and arthralgia.<sup>43,44</sup>

The radiological manifestations consist of patchy or confluent bilateral areas of consolidation due to diffuse pulmonary hemorrhage. The airspace consolidation tends to involve mainly the lower lung zones.<sup>44</sup>

### CONCLUSION

Imaging plays an important role in the initial evaluation and follow-up of patients with vasculitis. The most commonly utilized imaging modalities utilized in the evaluation of these patients are chest radiography and CT. The radiological findings, however, are variable and relatively nonspecific and need to be interpreted together with the clinical and laboratory findings.

### REFERENCES

1. Travis WF, Colby TV, Koss MN, Rosado-de-Christenson ML, Müller NL, King TE. *Nonneoplastic Disorders of the Lower Respiratory Tract*. Washington, DC: Armed Forces Institute of Pathology; 2002:233–264
2. Kuhlman JE, Hruban RH, Fishman EK. Wegener granulomatosis: CT features of parenchymal lung disease. *J Comput Assist Tomogr* 1991;15:948–952
3. Papis SA, Manoussakis MN, Drosos AA, et al. Imaging of thoracic Wegener's granulomatosis: the computed tomographic appearance. *Am J Med* 1992;93:529–536
4. Lee KS, Kim TS, Fujimoto K, et al. Thoracic manifestation of Wegener's granulomatosis: CT findings in 30 patients. *Eur Radiol* 2003;13:43–51
5. Cordier JF, Valeyre D, Guillevin L, et al. Wegener's granulomatosis: a clinical and imaging study of 77 cases. *Chest* 1990;97:906–912
6. Weir IH, Müller NL, Chiles C, et al. Wegener's granulomatosis: findings from computed tomography of the chest in 10 patients. *Can Assoc Radiol J* 1992;43:31–34
7. Sheehan RE, Flint JDA, Müller NL. Computed tomography features of thoracic manifestations of Wegener granulomatosis. *J Thorac Imaging* 2003;18:34–41
8. Maskell GF, Lockwood CM, Flower CDR. Computed tomography of the lung in Wegener's granulomatosis. *Clin Radiol* 1993;48:377–380
9. Foo S, Weisbrod GL, Herman SJ, Chamberlain DW. Wegener granulomatosis presenting on CT with atypical bronchovascular distribution. *J Comput Assist Tomogr* 1990;14:1004–1006
10. Stein MG, Gamsu G, Webb WR, Stulbarg MS. Computed tomography of diffuse tracheal stenosis in Wegener granulomatosis. *J Comput Assist Tomogr* 1986;10:868–870
11. Bohlman ME, Ensor RE, Goldman SM. Primary Wegener's granulomatosis of the trachea: radiologic manifestations. *South Med J* 1984;77:1318–1319
12. Daum TE, Specks U, Colby TV, et al. Tracheobronchial involvement in Wegener's granulomatosis. *Am J Respir Crit Care Med* 1995;151:522–526
13. Sreaton NJ, Sivasothy P, Flower CDR, Lockwood CM. Tracheal involvement in Wegener's granulomatosis: evaluation using spiral CT. *Clin Radiol* 1998;53:809–815
14. Shin MS, Yound KR, Ho K-J. Wegener's granulomatosis upper respiratory tract and pulmonary radiographic manifestations in 30 cases with pathogenetic consideration. *Clin Imaging* 1998;22:99–104
15. Ishikawa K. Diagnostic approach and proposed criteria for the clinical diagnosis of Takayasu's arteriopathy. *J Am Coll Cardiol* 1988;12:964–972
16. Kerr GS. Takayasu arteritis. *Ann Intern Med* 1994;120:919–929
17. Müller NL, Fraser RS, Colman N, Paré PD. *Radiologic diagnosis of diseases of the chest*. Philadelphia: WB Saunders; 2001:1515–1514
18. Park JH, Chung JW, Im J-G, et al. Takayasu arteritis: evaluation of mural changes in the aorta and pulmonary artery with CT angiography. *Radiology* 1995;196:89–93
19. Yamada I, Numano F, Suzuki S. Takayasu arteritis: evaluation with MR imaging. *Radiology* 1993;188:89–94
20. Takahashi K, Honda M, Furuse M, Yanagiasawa M, Saitoh K. CT findings of pulmonary parenchyma in Takayasu arteritis. *J Comput Assist Tomogr* 1996;20:742–748
21. Yamada I, Nakagawa T, Himeno Y, et al. Takayasu arteritis: diagnosis with breath-hold contrast-enhanced three-dimensional MR angiography. *J Magn Reson Imaging* 2000;11:481–487
22. Hara M, Goodman PC, Leder RA. FDG-PET finding in early-phase Takayasu arteritis. *J Comput Assist Tomogr* 1999;23:16–18
23. Churg J, Strauss L. Allergic granulomatosis, allergic angiitis and periarteritis nodosa. *Am J Pathol* 1951;27:277–301
24. Choi YH, Im J-G, Han BK, Kim J-H, Lee KY, Myoung NH. Thoracic manifestations of Churg-Strauss syndrome: radiologic and clinical findings. *Chest* 2000;117:117–124
25. Chumbley LC, Harrison EG Jr, DeRemee RA. Allergic granulomatosis and angiitis (Churg-Strauss syndrome): report and analysis of 30 cases. *Mayo Clin Proc* 1977;52:477–484
26. Lanham JG, Elkon KB, Pusey CD, et al. Systemic vasculitis with asthma and eosinophilia: a clinical approach to the Churg-Strauss syndrome. *Medicine* 1984;63:65–81
27. Worthy SA, Müller NL, Hansell DM, Flower CDR. Churg-Strauss syndrome: the spectrum of pulmonary CT findings in 17 patients. *AJR Am J Roentgenol* 1998;170:297–300
28. Buschman DL, Waldron JA, King TE. Churg-Strauss pulmonary vasculitis: high-resolution CT scanning and pathologic findings. *Am Rev Respir Dis* 1990;142:458–461

29. Erkan F, Cavdar T. Pulmonary vasculitis in Behçet's disease. *Am Rev Respir Dis* 1992;146:232-239
30. Raz J, Okon E, Chajek-Shaul T. Pulmonary manifestations in Behçet's syndrome. *Chest* 1989;95:585-589
31. Numan F, Islak C, Berkmen T, Tüzün H, Çokyüsel O. Behçet's disease: pulmonary arterial involvement in 15 cases. *Radiology* 1994;192:465-468
32. Ahn JM, Im J-G, Ryoo JW, et al. Thoracic manifestations of Behçet's syndrome: radiographic and CT findings in nine patients. *Radiology* 1995;194:199-203
33. Numan F, Islak C, Berkmen T, Tüzün H, Çokyüsel O. Behçet's disease: pulmonary arterial involvement in 15 cases. *Radiology* 1994;192:465-468
34. Tunaci A, Berkmen YM, Gokmen E. Thoracic involvement in Behçet's disease: pathological, clinical, and imaging features. *AJR Am J Roentgenol* 1995;164:51-56
35. Tunaci M, Ozkorkmaz B, Tunaci A, Gül A, Gülgün E, Acunas B. CT findings of pulmonary aneurysms during treatment for Behçet's disease. *Am J Roentgenol*; 1999;172:729-733
36. Puckette TC, Jolles H, Proto AV. Magnetic resonance imaging confirmation of pulmonary artery aneurysm in Behçet's disease. *J Thorac Imaging* 1994;9:172-175
37. Grenier P, Bletry O, Cornud F, et al. Pulmonary involvement in Behçet's disease. *AJR Am J Roentgenol* 1981;137:565-569
38. Kelly PT, Hapnik EF. Goopasture syndrome: molecular and clinical advances. *Medicine* 1994;73:171-185
39. Ball JA, Young K Jr. Pulmonary manifestations of Goodpasture's syndrome: antiglomerular basement membrane disease and related disorders. *Clin Chest Med* 1998;19:777-791
40. Bowley NB, Steiner RE, Chin WS. The chest x-ray in antiglomerular basement membrane antibody disease (Goodpasture's syndrome). *Clin Radiol* 1979;30:419-429
41. Müller NL, Miller RR. Diffuse pulmonary hemorrhage. *Radiol Clin North Am* 1991;29:965-971
42. Cheah FK, Sheppard MN, Hansell DM. Computed tomography of diffuse pulmonary hemorrhage with pathologic correlation. *Clin Radiol* 1993;48:89-93
43. Jennette JC, Falk RJ. Small-vessel vasculitis: proposal of an international speakers conference. *Arthritis Rheum* 1994;37:187-192
44. Lauque D, Cadranet J, Lazor R, et al. Microscopic polyangiitis with alveolar hemorrhage: a study of 29 cases and review of the literature. *Group d'etudes et de Recherche sur les Maladies "Orphelines" pulmonaires. Medicine (Baltimore)* 2000;79:222-233